Macromolecules **2005,** *38,* 8712–8718

Molecular Segregation in Polymer Melt Crystallization: Simulation Evidence and Unified-Scheme Interpretation

Wenbing Hu*

Department of Polymer Science and Engineering, State Key Laboratory of Coordination Chemistry, College of Chemistry and Chemical Engineering, Nanjing University, 210093, Nanjing, China

Received May 12, 2005; Revised Manuscript Received July 11, 2005

ABSTRACT: The segregation of the low-molecular-weight fractions on the crystal growth of polydisperse polymers has been identified as a general phenomenon by means of dynamic Monte Carlo simulations of lattice polymer systems. Its mechanism was elucidated on the basis of the intramolecular nucleation model. A unified scheme has been proposed to interpret all three scenarios of molecular segregation according to the location of the crystallization temperature T_c demarcated by two melting points of short-chain fractions, namely T_m^0 for the bulk extended-chain crystals and T_{m2D} for two-dimensional single-folded-chain crystals on a smooth crystal-growth front. In the first scenario, $T_c > T_m^0$, and short-chain fractions are thermodynamically forbidden in crystallization, like the small solvents in conventional monotectic polymer solutions. In the second scenario, $T_m^0 > T_c > T_{m2D}$, and short-chain fractions are fully excluded by their failures on the intramolecular secondary nucleation for folded-chain crystal growth. In the third scenario, $T_c \lesssim T_{m2D}$, and short-chain fractions are partially segregated due to their much less free energy gains in the intramolecular secondary nucleation than long-chain fractions. When $T_c \ll T_{m2D}$, both short-chain and long-chain fractions cocrystallize without any molecular segregation. In addition, an upper limit of molecular weights in crystallization fractionation has been explained.

I. Introduction

Crystallization of polymer chains usually involves close packing of molecules that is very sensitive to any mismatch in chemical structures. Segregation is, therefore, a common phenomenon in polymer crystallization. This is true especially when polymer chains contain irregularities of sequences such as different chemical species (including short branches), geometrical connections, or stereoisomers. However, the segregation occurs not only in the size scale of repeat units but also in much larger scales. For instance, a homogeneous distribution of irregular sequences among copolymer chains exhibits sequence-length segregation during crystallization,[1] while a heterogeneous distribution leads to a liquid–liquid phase separation driven by the component-selective crystallizability like in a polymer blend.[2] Nevertheless, even without any irregularities on the sequence, a polydispersity of molecular weights still gives rise to molecular segregation in polymer crystallization. For instance, since the melting point has a strong chain-length dependence at the short-chain end, it is easy to see the molecular segregation when the melting points of the short-chain fractions are lower than the crystallization temperature of the long-chain fractions. Furthermore, when the short-chain fractions are not so short and perform chain-folding crystallization, they undergo molecular segregation even below the equilibrium melting point, as observed in the experiments of polyethylene (PE) and poly(ethylene oxide) (PEO).[3,4] In the experiments, in addition to the above-mentioned thermodynamics scenario of molecular segregation, two more scenarios of molecular segregation have been observed in the supercooled regions, showing full segregation and partial segregation.[5–8] Thus far, however, the molecular segregation in the supercooled regions has not been further studied or been accepted as a general phenomenon for all other polymers. Recently, dynamic Monte Carlo simulations of lattice polymer systems have reproduced some basic facts of chain folding on polymer crystallization, such as the integer folding of short chains[9] as well as the chain-folding sectorization of single crystals.[10] An evidence of molecular simulations to identify the general phenomenon of molecular segregation in the supercooled regions is worthy of expectation, as will be the focus in this paper.

With respect to the interpretation, the chain-folding mechanism of polymer crystal growth is still a big challenge to our understanding.[11–13] Enlightened by the knowledge of small molecules, the well-known Lauritzen–Hoffman (LH) model has achieved many successes.[14–18] This model assumes that the rate of crystal growth is dominated by the secondary nucleation that is hindered mainly by the growth of the first crystalline stem on a smooth crystal-growth front. As a complement to explain the kinetics-controlled molecular segregation, Hoffman[19] has tried to consider the coexistence of a separate folded-chain nucleus with two free chain ends that bring an additional surface free energy penalty to the secondary nucleation. The similar idea has been discussed by Lindenmeyer and Peterson.[20] Thus, adding each new macromolecule on the crystal growth front may incur an additional difficulty, as proposed by Wunderlich and his collaborators in a speculative concept of molecular nucleation.[21–24] They assumed that the crystal growth of each new macromolecule must be initiated by a separate folded-chain secondary nucleation on the crystal-growth front. When the sizes of macromolecules are smaller than the critical unstable size of the nuclei, they will be excluded by the crystal growth of those higher-molecular-weight fractions. This concept provided deep insights and stimulated the recent proposition of the intramolecular nucleation (IN) model.[25] The IN model assumes that for long-chain polymers all the events of secondary nucleation are mainly initiated by the intramolecular chain-folding

---

* E-mail: wbhu@nju.edu.cn.

10.1021/ma050988n CCC: $30.25

process, and the criterion for molecular segregation is the critical stable size of nuclei that is larger than their critical unstable size. A quantitative interpretation to the kinetics-controlled molecular segregation can be obtained. In this paper, a unified scheme to interpret all three scenarios of molecular segregation, namely thermodynamics, kinetics, and rate competition, will be further proposed, for a specific fraction of molecular weights under variable crystallization temperatures from high to low, or equivalently, for a specific crystallization temperature with variable critical molecular weights from low to high.

In the following text, after a simple introduction to the simulation techniques, the molecular segregation in variable supercooled regions of a half-half-volume blend of 32-mers and 128-mers will be observed upon the isothermal crystal growth. The mechanism is elucidated in a detailed introduction of the IN model. Then, a unified scheme for the interpretation to all three scenarios of molecular segregation will be proposed. Furthermore, an upper limit of molecular weights in crystallization fractionation is explained. Finally, the paper ends up with some concluding remarks.

II. Simulation Techniques

A simple lattice model was employed in the dynamic Monte Carlo simulations, where polymer chains were “living” in a cubic box of 64^3 lattice with periodic boundary conditions. The microrelaxation of polymer chains allowed the single-site monomer to jump into a void neighbor, with partial sliding diffusion along the chain if necessary.[26] Meanwhile, double occupations and bond crossings were avoided to mimic the volume exclusion of polymers. 960 chains, each containing 128 monomers, and 3840 chains, each containing 32 monomers, were well mixed in the disordered coil states to construct a half−half volume blend. The polymer chains were fully flexible, and the mutual mixing between components of two chain lengths was athermal. In the conventional Metropolis sampling, the potential energy of parallel packing of neighboring bonds E_p was considered as the molecular driving force for crystallization.[27] Therefore, the system temperature was represented in a reduced form k_BT/E_p, where k_B was Boltzmann’s constant and T the temperature.

Since the high efficiency of molecular segregation can only be obtained in the crystal growth process rather than in the primary crystal nucleation, we focused our attention on the crystal growth only. To this end, we made the first 64 long chains (128-mers) fixed at once-folded extended conformations to form a double layer of terraced substrate. This substrate will induce polymer crystal growth under quite small supercoolings that are required for observing molecular segregation. The similar strategy to template crystal growth has been applied in the molecular simulations reported in ref 28.

In the following simulations, we first measured the equilibrium melting point of the pure 32-mers, and then we observed the molecular segregation on the crystal growth of the binary blend of 32-mers and 128-mers at the temperature below that melting point.

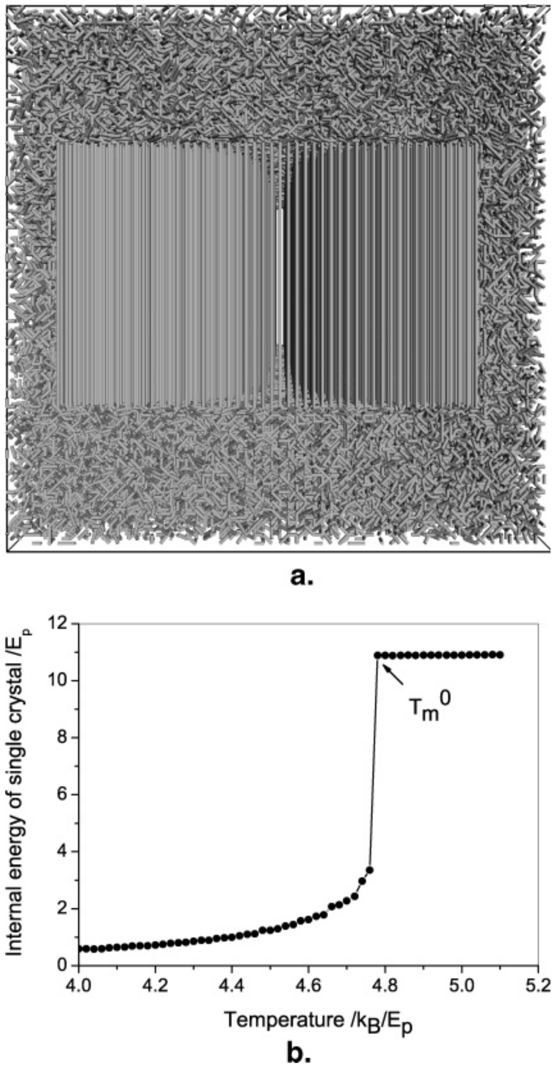

Figure 1. (a) Snapshot of the extended-chain single crystal (lateral size 50 × 64) embedded in the melt of 32-mers in a 64^3 cubic lattice with periodic boundary conditions. The occupation density is 0.9375. All the bonds are drawn in cylinders. (b) Heating curve of the internal energy of the single crystal showing the tentative equilibrium melting point $T_m^0 = 4.78E_p/k_B$.

III. Simulation Results

To make sure that the observation is made under a crystal-growth temperature supercooled for the short-chain fractions, it is first desirable to determine the equilibrium melting point of the short-chain fractions in our simulations. To this end, we prepared a single extended-32-mer crystal embedded in the melt of 32-mers, by simply rejecting all the trial moves of those crystalline chains on athermal annealing of the preset fully ordered state. The result is demonstrated by the snapshot in Figure 1a. After that, the restriction of mobility was removed, and the sample was heated with the step length of 0.02 in a smart program starting from $T = 4.00E_p/k_B$. The smart program decided a jump to the next temperature step after each block of 500 Monte Carlo (MC) cycles according to the internal energy of those chains belonging to the extended-chain crystal and showing the crystallization tendency. By this way, the overshooting of crystal melting induced by the fast temperature scanning can be diminished and the occurrence of melting transition can be sharpened. Here, the internal energy of the single crystal is defined as the mean number of nonparallel neighbors around each bond in the unit of E_p, and one MC cycle is defined as one trial move per monomer summed over all the monomers in the sample system. As shown in Figure 1b, the melting temperature occurs at $T_m^0 = 4.78E_p/k_B$,

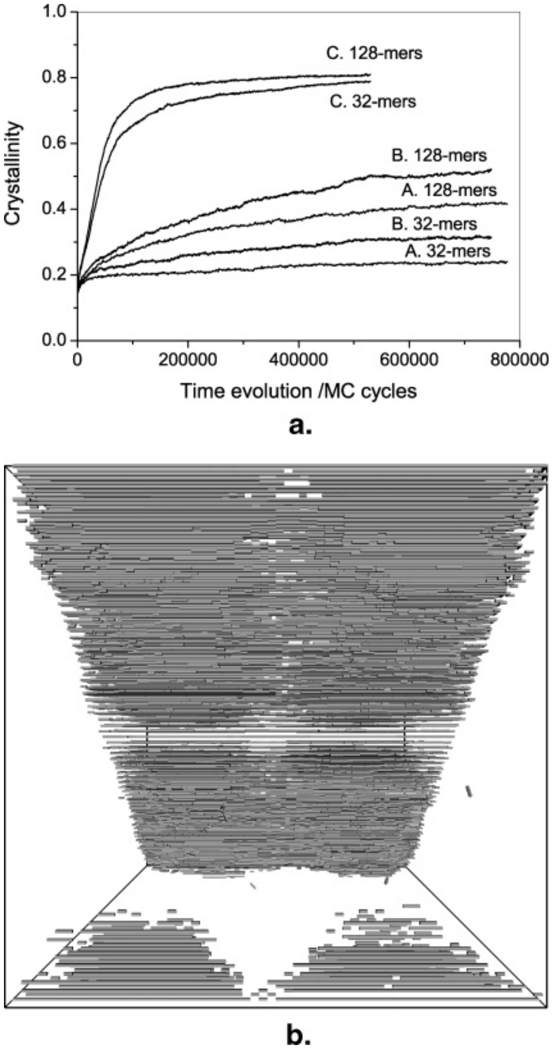

a.

b.

Figure 2. (a) Time evolution of the paired crystallinity curves corresponding to two chain lengths at the crystal growth temperatures of (A) $4.5E_p/k_B$, (B) $4.45E_p/k_B$, and (C) $4.2E_p/k_B$. The sample system is a half−half volume blend of two chain lengths (32-mers and 128-mers) in a 64^3 cubic lattice with periodic boundary conditions, and a terrace substrate formed by 128-mers exists to initiate the crystal growth under low supercoolings. (b) Snapshot of 128-mer crystals grown at the temperature of $4.5E_p/k_B$. In addition to the double-layer terraced substrate, only the bonds containing more than 10 parallel neighbors are shown in cylinders.

which can be regarded as the tentative equilibrium melting point of 32-mers in our simulations.

Then, to observe the molecular segregation on the crystal growth of the binary blend, we chose the supercooled temperature at $4.5E_p/k_B$. The results are shown in Figure 2a. In this figure, the crystallinities that are defined as the mean fraction of bonds containing more than five parallel neighbors are calculated for two fractions of chain lengths separately. They indeed show that in the limited time window of our observation only the long-chain fraction is crystallizable at this temperature. The baseline crystallinity of the short-chain fractions at about 0.2 can be mainly attributed to the thermal fluctuations and substrate adsorption in the supercooled melt. However, at the slightly lower temperature $4.45E_p/k_B$, the short-chain fraction can crystallize a little but much slower than the long-chain fraction, as shown also in Figure 2a. In this case, further crystallization of the short-chain fraction seems to require new events of primary crystal nucleation. Under even lower temperatures such as $4.2E_p/k_B$, both fractions of chain lengths cocrystallize although the short-chain fraction reaches at a slightly lower crystallinity with a slightly lower speed. Therefore, under the chosen three supercoolings for the short-chain fractions, three pairs of crystallinity curves in Figure 2a demonstrate full segregation, partial segregation, and no segregation, respectively, in accordance with the experimental observations on PE and PEO.[5−8]

Molecular simulations have the advantage to see the molecular details of crystal morphologies. We, therefore, made the snapshot of long-chain crystals grown at the temperature of $4.5E_p/k_B$, as shown in Figure 2b. From this figure, one can see that the long-chain fractions are in priority of the crystal growth on both sides of the terraced substrate. The crystal growth front appears clearly wedge-shaped. It is ready to imagine that the very slow secondary nucleation at this temperature can be mainly attributed to the slow reorganization of the highly folded chains at the tip of crystal growth front. The small size of wedge tips inhibits further secondary crystal nucleation upon it. A typical case of such has been found as the so-called self-poisoning for the crystal growth of the extended chains inhibited by the metastable once-folded chains on the crystal growth front.[29]

IV. Intramolecular Nucleation Model

To interpret the above simulation results, the IN model should be introduced first. This model assumes that in a long-chain system both primary and secondary crystal nucleations are dominated by the intramolecular correlation of the chain units.[25] It should be considered that in the melt polymer coils are interpenetrated into each other, and some other chains may be involved into the nucleation events of a single chain. We do not prefer to reject the coexistence of the intermolecular nucleation that should be dominant in the crystallization of very short chains and in particular, of small molecules. But here, for the chain-folding crystallization of long-chain samples, we suppose that in thermal/density fluctuations those nucleation events are mainly activated by the strong intramolecular correlation of one chain, and the other chains are involved rather passively. Therefore, we focus our attention only on the crystallization and melting of a single chain and neglect the disturbance of involving other chains at this moment.

Following the classical crystal-nucleation theory[30,31] except that we regard a fully extended chain embedded in the bulk crystalline phase as the ground state, the free energy of a single chain can be estimated according to the body free energy change due to partial melting plus a surface free energy penalty, as given by[25]

$$\Delta F_{3D}(n) = n\Delta f_{3D} + \sigma_{3D}(N - n)^{2/3} \tag{1}$$

where n is the number of molten bonds, Δf_{3D} the body free energy change of each bond on melting, σ_{3D} a constant corresponding to the surface free energy density and absorbing all the prefactors, and N the total amount of bonds in the single chain. In previous simulations,[25] the molten bonds have been defined as those bonds containing less than five parallel neighbors. Equation 1 estimates the free energy of the single chain on the basis of one single crystal for primary nucleation.

In the case of secondary nucleation, the single chain forms a single two-dimensional crystal on a locally smooth crystal-growth front. The smoothness may not be a strict prerequisite of the following free energy estimation, since the intramolecular nucleus covering over a step of terrace on the crystal growth front may not change the result much. Similarly, the total free energy of this single chain is estimated according to a body free energy change due to partial melting plus a lateral surface free energy penalty, as given by[25]

$$\Delta F_{2D}(n) = n\Delta f_{2D} + \sigma_{2D}(N - n)^{1/2} \qquad (2)$$

The free energy barrier for intramolecular primary nucleation is thus calculated as

$$\Delta F_{c3D} = \frac{4{\sigma_{3D}}^{3}}{27{\Delta f_{3D}}^{2}} \qquad (3)$$

The validity of this equation has been quantitatively verified by our previous molecular simulations.[25] Since Δf_{3D} is roughly proportional to the supercooling, this equation predicts that the height of free energy barrier has a reciprocal dependence on the square of supercooling. This result is well-known for the homogeneous primary crystal nucleation and in agreement with experimental observations on real polymers.[32] Furthermore, this equation shows that under a fixed temperature (fixed Δf_{3D}) the height of free energy barrier should be independent of the chain length. This result is also consistent with recent experimental observations on both extended-chain crystals and folded-chain crystals of PE[33,34] as well as on the primary crystal nucleation of polyethylene succinate.[35]

Correspondingly, the free energy barrier for intramolecular secondary nucleation is calculated as

$$\Delta F_{c2D} = \frac{{\sigma_{2D}}^{2}}{4\Delta f_{2D}} \qquad (4)$$

which predicts not only a reciprocal dependence on the supercooling as already well-known but also an independence on the chain length at a fixed temperature. It has been verified in experiments that the free energy barrier for secondary crystal nucleation of polymers has a reciprocal dependence on the supercooling.[36] The chain-length independence of the critical free energy barrier for crystal growth can also be verified by the crystal growth rates of polyethylene succinate.[37,38]

For the molecular segregation under supercooling, we will focus our attention on the secondary nucleation since as mentioned before, the primary nucleation involves only a little polymers and hence cannot provide the high efficiency of molecular segregation. Opposite to the secondary nucleation, the free energy barrier for melting of single chains on the crystal-growth front is

$$\Delta F_{m2D} = N\Delta f_{2D} - \sigma_{2D}N^{1/2} + \frac{{\sigma_{2D}}^{2}}{4\Delta f_{2D}} \qquad (5)$$

which shows a significant chain-length dependence. This implies that, under a specific crystallization temperature, ΔF_{c2D} is invariable while ΔF_{m2D} is variable with the chain length. In this case, there should exist a critical chain length N_c which meets the condition of height equivalence between two free energy barriers of opposite directions. This equivalence indicates the thermodynamic equilibrium between crystalline and molten states. Therefore, those chains shorter than this critical chain will have the crystalline state less stable than the molten state and hence have a potentiality to dissolve/melt from the crystal growth front, and those chains longer than this critical chain can survive in the intramolecular secondary nucleation and contribute to the advancing of the crystal-growth front. The depicted free energy curves with variable chain lengths can be found in Figure 3. This simple description reveals the principle of kinetics-controlled molecular segregation on polymer crystal growth.

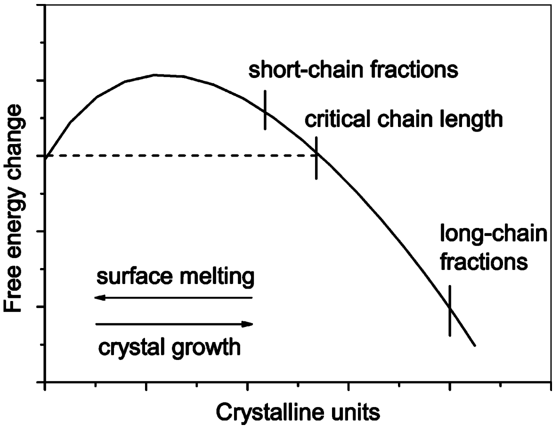

Figure 3. Depicted free energy curves for the secondary nucleation of single chains with variable chain lengths on the smooth crystal growth front. The dashed line indicates the equilibrium condition at the critical chain length.

For those chains of critical chain lengthes, the thermodynamic equilibrium between two states defines their equilibrium melting point T_{m2D} at this specific crystallization temperature. Applying this equilibrium condition into eqs 4 and 5, we have

$$\Delta f_{e2D} = \sigma_{2D}{N_c}^{-1/2} \qquad (6)$$

This equation tells us that the higher the crystallization temperature, the larger the critical chain length. Therefore, on cooling of a highly polydisperse polymer melt, the long-chain fractions that meet the critical condition first will crystallize at high temperatures and contribute to the thick dominant lamellae, while the short-chain fractions only crystallize at low temperatures and contribute dominantly to the thin subsidiary lamellae. This explains the corresponding observations in experiments.[39,40] Furthermore, the scaling relationship (−1/2) between the crystallization temperature and the critical chain length of molecular fractionation has been verified by the experimental data obtained from PE melt crystallization.[25]

The measurement of a total chain length on the crystal-growth front is actually an extreme case of the IN model. In most of cases, the intramolecular nucleation is not necessary to know the exact distance of chain ends along a long chain, but rather to make certain that they are outside the critical distance along the chain. In thermal fluctuations of a long-chain macromolecule, finding both chain ends requires the correlation length larger than the coil size, while finding the critical chain length is in a much smaller and reasonable scale. Thus, only a small portion of chain that reaches the critical chain length may be involved in the nucleation events for advancing the crystal-growth front. After the secondary nucleation is finished, the crystal growth along the chain spreads over the smooth substrate but may not always complete at the chain ends. Many factors will contribute to the termination of this spreading process, such as a finite size of the crystal-growth front as has already been observed in our previous simulations.[10] The others can be the impingements with other surface crystallites or the feeding restrictions by slow long-chain disentanglements in the melt. After the termination, the rest molten part of single chains may be still long enough to make another event of secondary nucleation. Therefore, a long-chain macromolecule is expected to perform crystal growth in an intermittent style and with many events of intramolecular nucleation.[10]

Many recent observations contain certain supportive implications to the IN model. In a visual inspection of molecular dynamics simulations, Meyer and his collaborator found that intrachain nuclei were mostly the starting point of crystal growth.[41] By means of Brownian dynamics simulations, Muthukumar's group has analyzed the dynamics to generate several primary crystal nuclei simultaneously along a single chain,[42] although multiple nucleation usually occurs at low temperatures and they focused their attention on the entropic barrier sourced from those connecting loops. Under the dynamics point of view, each IN event can be reversible. This behavior may give rise to many local reversals on the crystal growth front[9] and hence makes contributions to the reversible heat capacity of semicrystalline macromolecules as reported in Wunderlich's group.[43] Quenching the highly polydisperse sample to low temperatures, the smaller critical chain length allows cocrystallization of more chain-length fractions, as summarized in Gedde's book.[44] In this case, a very-long-chain macromolecule may contain quite a few of intramolecular nuclei, and therefore, in the contexture of semicrystalline polymers, the trajectory of such a macromolecule may travel over several thin lamellae or several positions in the same lamella, without a significant sacrifice of the coil-size scaling in the melt.

V. Unified Scheme for Interpretation of Molecular Segregation

As summarized in the Introduction, there are three scenarios of molecular segregation observed in experiments. The first scenario exhibits the melting point T_m^0 of the short-chain fractions beneath the crystallization temperature of the long-chain fractions, so the short-chain fractions are forbidden to perform crystallization by the thermodynamical driving forces and behave like the small solvent in the conventional monotectic polymer solutions. The second one requires chain folding upon crystal growth, and the molecular segregation is decided by the chain length compared to a critical chain length with its two-dimensional melting point T_{m2D} located at the crystallization temperature, as introduced in the above section. Since two-dimensional crystals on the smooth growth front are much less stable than the bulk extended-chain crystals (i.e., $T_{m2D} \ll T_m^0$), the second scenario of molecular segregation occurs under a supercooling of the segregated short-chain fractions. The third scenario shows only partial segregation and can be assigned to the temperature region below but near T_{m2D}, where the free energy gains of short-chain fractions on the intramolecular secondary nucleation are much smaller than those of long-chain fractions. In other words, crystal growth by short-chain fractions contains a high probability of reversal while crystal growth by long-chain fractions has no reversal. Therefore, as a consequence of the growth-rate competition, the former will be gradually excluded from the crystal growth front although the former may be still crystallizable at later stages of crystallization. On further lowering of the crystallization temperature, both fractions will cocrystallize without any segregation.

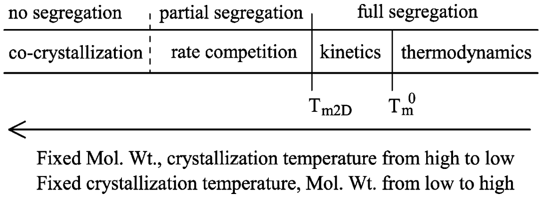

Figure 4. Demonstration of a unified scheme to interpret three scenarios of molecular segregation in polymer crystallization. The first text line shows the status of molecular segregation, and the second line shows the scenarios of molecular segregation. Below is the unified scheme according to the crystallization temperature or alternatively, according to the critical molecular weight.

On the basis of the above analysis, we may construct a unified scheme to describe all three scenarios, namely thermodynamics, kinetics, and rate competition, according to the location of the crystallization temperature demarcated by T_m^0 and T_{m2D} for a specific molecular weight. An alternative choice is the location of the critical molecular weight demarcated by its values corresponding to two melting points equal to a specific crystallization temperature. In the polydisperse polymer with a wide molecular weight distribution, the shortest chains perform thermodynamics scenario of molecular segregation and the middle-length chains exhibit kinetics scenario, while the longer chains are in partial segregation or even in cocrystallization. A demonstration of this unified scheme is shown in Figure 4.

In the practical molecular fractionation, T_m^0 plays a dominant role only in the chain-extending crystallization of very short chains, while T_{m2D} is meaningful in the chain-folding crystallization of those long chains. Therefore, T_{m2D} is of practical importance in the crystallization fractionation of conventional high polymers, with the crystallization temperature scanning from high to low for obtaining the variable fractions of molecular weights. In the following section, T_{m2D} will be employed to explain an upper limit of molecular weights in crystallization fractionation.

VI. Upper Limit of Molecular Weights in Crystallization Fractionation

There exists even an upper limit of molecular weights in the chain-folding crystallization fractionation first suggested by Mehta and Wunderlich[22] and then confirmed by Glaser and Mandelkern[45] in their experiments of PE melt crystallization. Crystallization in a polydisperse polymer with all the chain lengths going beyond this upper limit will not exhibit molecular segregation anymore.

As will be proved below, this upper limit is still an inherent prediction of the IN model. According to the basic thermodynamic expression $\Delta f_{e2D} = \Delta h_{e2D} - T_{m2D}\Delta s_{e2D}$, where Δh is the fusion enthalpy per chain unit and Δs the fusion entropy per chain unit, we can obtain from eq 6 that

$$T_{\mathrm{m2D}} = \frac{\Delta h_{\mathrm{e2D}} - \sigma_{\mathrm{2D}} N_{\mathrm{c}}^{-1/2}}{\Delta s_{\mathrm{e2D}}} \qquad (7)$$

At this equilibrium melting temperature, the free energy barrier is given by

$$\Delta F_{\mathrm{e2D}} = \frac{\sigma_{\mathrm{2D}}^{2}}{4\Delta f_{\mathrm{e2D}}} = \frac{\sigma_{\mathrm{2D}}}{4} N_{\mathrm{c}}^{1/2} \qquad (8)$$

Supposing that the critical chain length approaches infinity, eq 7 implies that T_{m2D} will be saturated at a definite value ($\Delta h_{\mathrm{e2D}}/\Delta s_{\mathrm{e2D}}$), while eq 8 shows that ΔF_{e2D} will eventually go to infinity.

It is well-known that only when the thermal energy approaches the free energy barrier can the spontaneous events of nucleation/melting occur on the crystal-growth front. The thermal energy has a proportional dependence on the temperature (here, T_{m2D}). This relationship implies that when the critical chain length goes to infinity, the thermal energy will eventually reach a definite value rather than infinity. Therefore, there should exist an upper limit of the critical chain length, above which the thermal energy will never catch up with the free energy barrier that intends to increase with the chain length up to infinity. Beyond that limit, no polymer will be spontaneously excluded from the crystal-growth front by the reverse of secondary nucleation, and hence the phenomenon of molecular segregation disappears.

To give a demonstrative estimation of this upper limit, we draw the parameters from the lattice model of polymer chains described in ref 25 and apply them to eqs 7 and 8. We assume a lattice polymer chain performing two-dimensional secondary crystal nucleation/melting on a smooth crystal-growth front. The normal direction of this front shall be aligned with one of lattice axes. According to the applied microrelaxation model in our simulations, the coordination number of each lattice site (or each chain bond) includes all the neighbors along the lattice axes (6) and the body (8) and face (12) diagonals, and hence $q = 6 + 8 + 12 = 26$. Therefore, each chain bond melting from the front will lose the potential energy from its crystalline interactions with nine neighbors belonging to the front, and their sum is $9E_{\mathrm{p}}$. In addition, the melting bond will lose the potential energy from its crystalline interactions with eight neighbors belonging to its layer just above the front, and their sum is $8E_{\mathrm{p}}/2$. Here, "2" is the symmetric factor for pair interactions of the bonds belonging to the concerning single chain. Thus, the fusion enthalpy of each bond is their total, $9 + 4 = 13E_{\mathrm{p}}$. The fusion entropy of each chain bond is still conformational in majority, and in analogy to a random walk it gives $k_{\mathrm{B}} \ln(q - 1)$.[25] So far so good; the last parameter in eq 7 needed to be specified is σ_{2D}. In the case of primary nucleation, the simulation results for the free energy barrier of equilibrium melting in a single chain have been fitted well by a single value $\sigma_{\mathrm{3D}} = 15E_{\mathrm{p}}$.[25] Assuming that three-dimensional crystal nuclei have a geometrical prefactor of 6 (cubic) and two-dimensional ones have a geometrical prefactor of 4 (square), a reasonable value of σ_{2D} is then $\sigma_{\mathrm{3D}}(4/6) = 10E_{\mathrm{p}}$. Taking all the available parameters into eq 7, we have

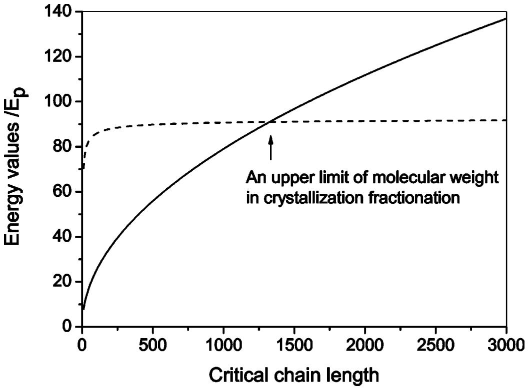

Figure 5. Demonstration of a crossover between two curves. The solid curve is for the equilibrium free energy barrier $\Delta F_{\mathrm{e2D}}/E_{\mathrm{p}}$ vs the critical chain length N_{c}, and the dashed curve is for the available thermal energy at the equilibrium melting temperature $10k_{\mathrm{B}}T_{\mathrm{m2D}}/E_{\mathrm{p}}$ vs N_{c}. For the details of calculations, see the text.

$$k_{\mathrm{B}}T_{\mathrm{m2D}}/E_{\mathrm{p}} = (13 - 10N_{\mathrm{c}}^{-1/2})/\ln(25) \qquad (9)$$

Within an acceptable time window of our simulations, the thermal energy has been found to be about $10k_{\mathrm{B}}T$.[25] Therefore, under the variable critical chain lengths, we compare the available thermal energy $10k_{\mathrm{B}}T_{\mathrm{m2D}}$ with the equilibrium free energy barrier ΔF_{e2D} calculated from eq 8, as shown in Figure 5.

Figure 5 clearly demonstrates a crossover between two curves. This crossover indicates an upper limit of the critical chain length above which the thermal energy will never catch up with the melting barrier; hence, the spontaneous molecular segregation between different length polymer chains will not occur. In other words, those short-chain fractions are not short enough and will never be spontaneously excluded from the crystal growth front. Actually at their T_{m2D}, the free energy barrier turns out to be so high that even secondary crystal nucleation cannot spontaneously happen anymore.

The exact molecular weight of this upper limit is still controversial in experiments of PE melt crystallization. Glaser and Mandelkern suggested a value at about 7700 Da,[45] while Mehta and Wunderlich showed their expectations for the molecular segregation on at least 2.2 × 10^4 Da.[22] In the present case, Figure 5 predicts an upper limit of the critical chain length at about 1326 bonds. This value corresponds to the molecular weight 1.9 × 10^4 Da of PE. It is obvious that the exact molecular weight of this upper limit depends on the details of experimental and theoretical approaches, especially on the time windows of observations. In fact, Sadler[46] has already observed that the molecular segregation of long chains happens very slowly at high crystallization temperatures. At even higher temperatures, the time scale required for the observation of molecular segregation becomes too large to be accepted by experiments. Moreover, Pennings[47] found that a proper stirring will make the high-molecular-weight fraction crystallize in priority. The high orientation of chains in the melt will decrease the fusion entropy and hence raises the equilibrium melting temperature. There are two aspects for the role of raising melting point in the acceleration of molecular segregation. First, the effective supercooling (the thermodynamical driving force) for crystallization of those long chains is enhanced since their oriented states can survive over a long term. Second, the crossover point in Figure 5 will shift up since the thermal energy increases with the equilibrium melting point of those oriented chains while the equilibrium barrier will not; hence, we expect to see that the molecular segregation is allowed to occur at higher temperatures for separating the fractions of longer chains.

VII. Concluding Remarks

Molecular simulations are powerful tools to evidence the general phenomenon of the molecular segregation on polymer crystal growth. Its mechanism can be well explained on the basis of the IN model. Furthermore, all three scenarios of molecular segregation can be interpreted under a unified scheme, as proposed in this paper.

Molecular segregation in supercooled regions is a unique phenomenon for polymer crystallization and thus implies a different crystallization mechanism of polymers from that of small molecules. The IN model inherits the concept of molecular nucleation and has assigned this uniqueness to the chain folding that is initiated mainly through the events of intramolecular primary and secondary nucleations.

A very special case of molecular segregation exists in the blend of normal and deuterated polymers.[48] The nature of this isotopic effect can be attributed to a small volume difference of repeat units.[49] Thermodynamic slowing down of interdiffusion has been found at the critical composition of demixing.[50] To some extent, this behavior ruined the success of small-angle neutron scattering measurements on polymer crystallization at high temperatures. Here, in the discussion of molecular segregation upon polymer crystallization, we leave this potential contribution alone.

In this paper, we mainly discuss the term of critical free energy barrier in the classical rate equation of crystal nucleation. Many experimental observations on the basic facts of polymer crystallization can be predicted according to the properties of this term. Our discussions can be compatible with other discussions focusing on other terms in the rate equation and later stages of crystallization, such as the prefactor of the barrier term that has been found responsible for the molecular diffusivity in the melt (see refs 17, 18, and 33−37), the reorganization on the crystal growth front including thickening or even a mesomorphic phase transition accompanied,[51,52] and so on.

Acknowledgment. The author is indebted much to Prof. Leo Mandelkern and Prof. Bernhard Wunderlich for their kindly encouragement and stimulative discussions. The financial support of his research from Nanjing University (Talent Introducing Fund No. 0205004108 and 0205004215), from Department of Education of China (Plan to Support New-Century Excellent Talent), and from National Natural Science Foundation of China (NSFC Grant No. 20474027) is appreciated, too.

References and Notes

(1) Hu, W.-B.; Mathot, V. B. F. *Macromolecules* **2004**, *37*, 673.
(2) Hu, W.-B.; Mathot, V. B. F. *J. Chem. Phys.* **2003**, *119*, 10953.
(3) Wunderlich, B. *Macromolecular Physics*; Academic Press: New York, 1976; Vol. 2, Chapter 5.3, p 88.
(4) Gedde, U. W. *Polymer Physics*; Chapman and Hall: London, 1995; p 189.
(5) Cheng, S. Z. D.; Wunderlich, B. *J. Polym. Sci., Part B: Phys. Ed.* **1986**, *24*, 577.
(6) Cheng, S. Z. D.; Wunderlich, B. *J. Polym. Sci., Part B: Phys. Ed.* **1986**, *24*, 595.
(7) Cheng, S. Z. D.; Bu, H.-S.; Wunderlich, B. *J. Polym. Sci., Part B: Phys. Ed.* **1988**, *26*, 1947.
(8) Gedde, U. W. *Prog. Colloid Polym. Sci.* **1992**, *87*, 8.
(9) Hu, W.-B. *J. Chem. Phys.* **2001**, *115*, 4395.
(10) Hu, W.-B.; Frenkel, D.; Mathot, V. B. F. *Macromolecules* **2003**, *36*, 549.
(11) Armistead, K.; Goldbeck-Wood, G. *Adv. Polym. Sci.* **1992**, *100*, 219.
(12) Wunderlich, B. In *Crystallization of Polymers*; Dosiere, M., Ed.; Kluwer: Dordrecht, 1993; p 236.
(13) Cheng, S. Z. D.; Lotz, B. *Philos. Trans. R. Soc. London A* **2003**, *361*, 517.
(14) Lauritzen, J. I.; Hoffman, J. D. *J. Res. Natl. Bur. Stand., Sect. A* **1960**, *64*, 73.
(15) Hoffman, J. D.; Lauritzen, J. I. *J. Res. Natl. Bur. Stand., Sect. A* **1961**, *65*, 297.
(16) Hoffman, J. D.; Davis, G. T.; Lauritzen, J. I. In *Treatise on Solid State Chemistry*; Hannay, N. B., Ed.; Plenum Press: New York, 1976; Vol. 3, p 497.
(17) Hoffman, J. D.; Miller, R. L. *Polymer* **1997**, *38*, 3151.
(18) Armistead, J. P.; Hoffman, J. D. *Macromolecules* **2002**, *35*, 3895.
(19) Hoffman, J. D. *SPE Trans* **1964**, *4*, 315. See also ref 3.
(20) Lindenmeyer, P. H.; Peterson, J. M. *J. Appl. Phys.* **1968**, *39*, 4929.
(21) Wunderlich, B.; Mehta, A. *J. Polym. Sci., Part B: Polym. Phys.* **1974**, *12*, 255.
(22) Mehta, A.; Wunderlich, B. *Colloid Polym. Sci.* **1975**, *253*, 193.
(23) Wunderlich, B. *Faraday Discuss.* **1979**, *68*, 239.
(24) Cheng, S. Z. D.; Wunderlich, B. *Macromolecules* **1989**, *22*, 1866.
(25) Hu, W.-B.; Frenkel, D.; Mathot, V. B. F. *Macromolecules* **2003**, *36*, 8178.
(26) Hu, W.-B. *J. Chem. Phys.* **1998**, *109*, 3686.
(27) Hu, W.-B. *J. Chem. Phys.* **2000**, *113*, 3901.
(28) Hu, W.-B.; Frenkel, D.; Mathot, V. B. F. *J. Chem. Phys.* **2003**, *118*, 10343.
(29) Ungar, G. *Crystallization of Polymers*; Dosiere, M., Ed.; Kluwer: Dordrecht, 1993.
(30) Gibbs, J. W. *The Scientific Work of J. Willard Gibbs*; Longmans Green: New York, 1906; Vol. 1, p 219.
(31) Volmer, M.; Weber, A. *Z. Phys. Chem. (Munich)* **1926**, *119*, 227.
(32) See ref 3, Chapter 5.1, p 1.
(33) Nishi, M.; Hikosaka, M.; Ghosh, S. K.; Toda, A.; Yamada, K. *Polym. J.* **1999**, *31*, 749.
(34) Ghosh, S. K.; Hikosaka, M.; Toda, A. *Colloid Polym. Sci.***2001**, *279*, 382.
(35) Umemoto, S.; Hayashi, R.; Kawano, R.; Kikuntani, T.; Okui, N. *J. Macromol. Sci.* **2003**, *B42*, 421.
(36) Umemoto, S.; Okui, N. *Polymer* **2002**, *43*, 1423.
(37) Umemoto, S.; Okui, N. *J. Macromol. Sci.* **2002**, *B41*, 923.
(38) See ref 3, Chapter 5.2, p 72.
(39) Bassett, D. C. *Principles of Polymer Morphology*; Cambridge University Press: Cambridge, 1981; p 103.
(40) See ref 4, p 147.
(41) Meyer, H.; Mueller-Plathe, F. *Macromolecules* **2002**, *35*, 1241.
(42) Muthukumar, M.; Welch, P. *Polymer* **2000**, *41*, 8833.
(43) Wunderlich, B. *Prog. Polym. Sci.* **2003**, *28*, 383.
(44) See ref 4, p 151.
(45) Glaser, R. H.; Mandelkern, L. *J. Polym. Sci., Part B: Polym. Phys.***1988**, *26*, 221.
(46) Sadler, D. M. *J. Polym. Sci., Part A* **1971**, *2*, 779.
(47) Pennings, A. J. *J. Polym. Sci., Part C* **1967**, *16*, 1799.
(48) Bates, F. S.; Wignall, G. D.; Koehler, W. C. *Phys. Rev. Lett.* **1985**, *55*, 2425.
(49) Buckingham, A. D.; Henschel, H. G. E. *J. Polym. Sci., Part B: Polym. Phys.* **1980**, *18*, 853.
(50) Green, P. F.; Doyle, B. L. *Phys. Rev. Lett.* **1986**, *57*, 2407.
(51) Keller, A.; Hikosaka, M.; Rastogi, S.; Toda, A.; Barham, P. J.; Goldbeck-Wood, G. *J. Mater. Sci.* **1994**, *29*, 2579.
(52) Strobl, G. *Eur. Phys. J. E* **2000**, *3*, 165.

MA050988N